

QCD string in light-light and heavy-light mesons

Yu.S.Kalashnikova^{*a}, A.V.Nefediev^{** a,b}, Yu.A.Simonov^{*** a}

^a*Institute of Theoretical and Experimental Physics, 117218,*

B.Chermushkinskaya 25, Moscow, Russia

^b*Centro de Física das Interações Fundamentais (CFIF), Departamento de Física,*

Instituto Superior Técnico, Av. Rovisco Pais, P-1049-001 Lisboa, Portugal

Abstract

The spectra of light–light and heavy–light mesons are calculated within the framework of the QCD string model, which is derived from QCD in the Wilson loop approach. Special attention is paid to the proper string dynamics that allows us to reproduce the straight-line Regge trajectories with the inverse slope being $2\pi\sigma$ for light–light and twice as small for heavy–light mesons. We use the model of the rotating QCD string with quarks at the ends to calculate the masses of several light-light mesons lying on the lowest Regge trajectories and compare them with the experimental data as well as with the predictions of other models. The masses of several low-lying orbitally and radially excited heavy–light states in the D , D_s , B , and B_s meson spectra are calculated in the einbein (auxiliary) field approach, which has proven to be rather accurate in various calculations for relativistic systems. The results for the spectra are compared with the experimental and recent lattice data. It is demonstrated that an account of the proper string dynamics encoded in the so-called string correction to the interquark interaction leads to an extra negative contribution to the masses of orbitally excited states that resolves the problem of the identification of the $D(2637)$ state recently claimed by the DELPHI Collaboration. For the heavy-light system we extract the constants

^{*}yulia@heron.itep.ru ^{**}nefediev@cfif.ist.utl.pt ^{***}simonov@heron.itep.ru

$\bar{\Lambda}$, λ_1 , and λ_2 used in Heavy Quark Effective Theory (HQET) and find good agreement with the results of other approaches.

PACS: 12.38.Aw, 12.39.Hg, 12.39.Ki

I. INTRODUCTION

The description of the mass spectrum of hadrons is one of the fundamental problems of strong interactions. It has been attacked in a sequence of approaches motivated by QCD, but still attracts considerable attention. One of the most intriguing phenomena — namely, the formation of an extended object, the QCD string, between the colour constituents inside hadrons, — plays a crucial role in understanding their properties. In the present paper this role is exemplified by spectra of the mass of light-light and heavy-light mesons. In the former case we study the role played by the QCD string in formation of the straight-line Regge trajectories and discuss the form of the interquark interaction inside light hadrons. For heavy-light mesons we find the masses of several low-lying states in the D , D_s , B , and B_s meson spectra including orbitally and radially excited ones.

We calculate and discuss the spin-spin and spin-orbit splittings and compare them to experimental and recent lattice data. Special attention is paid to the role of the proper string dynamics in establishing the correct slope of the Regge trajectories for both light-light and heavy-light states, as opposed to those following from relativistic equations with local potentials.

We remind the reader then that an extra piece of the effective interquark potential, the string correction, which is entirely due to the string-type interaction in QCD [1,2], gives a negative contribution to the masses of orbitally excited states. The latter observation allows us to resolve the “mystery” of an extremely narrow $D(2637)$ state (and a similar one in the B -mesonic spectrum) [3] recently claimed by the DELPHI Collaboration [4,5]. We present a reasonable fit for the several lowest states in D - and B -mesonic spectra using the standard

values for the string tension, the strong coupling constant, and the current quark masses. We also find the correspondence between our model and Heavy Quark Effective Theory, extracting the constants used in the latter approach in the expansion of a heavy-light meson mass in the inverse powers of the heavy quark mass. We find analytical formulae for these constants and compare their numerical estimates with the predictions of other models.

The two main approaches used in the numerical calculations are the quasiclassical method of solving the eigenenergies problem and the variational one based on the einbein field formalism. The accuracy of both methods is tested using exactly solvable equations and found to be about 7% at worst even for the lowest states. Possible improvements of the method are outlined and discussed.

The paper is organized as follows. In Section II we give a brief insight into various aspects of the einbein field formalism. In Section III the exact spectra of relativistic equations are compared to the results of approximate calculations using the quasiclassical and variational einbein field methods, as well as the combined one. In Section IV we discuss the problem of the Regge trajectory slopes as they appear from the relativistic equations with local potentials and from the string-like picture of confinement. Derivation of the Hamiltonian for the spinless quark-antiquark system as well as of the spin-dependent corrections to it is the subject of Section V. The spectra of light-light and heavy-light mesonic states are calculated and discussed in Sections VI and VII, respectively. Section VIII contains our conclusions and outlook.

II. EINBEIN FIELD FORMALISM

In this section we give a short introduction to the method of einbein fields and its possible applications to relativistic systems. The interested reader can find a more detailed information in [6] and references therein.

A. Reparametrization invariance and constrained systems

Historically the einbein field formalism was introduced in [7] to treat the kinematics of the relativistic spinless particles. Later it was generalized to the case of spinning particles [8] and strings [9]. So the action of a free relativistic particle can be rewritten as¹

$$S = \int_{\tau_i}^{\tau_f} L(\tau), \quad L = -m\sqrt{\dot{x}^2} \rightarrow -\frac{m^2}{2\mu} - \frac{\mu\dot{x}^2}{2}, \quad (1)$$

where the dot denotes derivative with respect to the proper time τ , μ being the einbein field². The original form of the action can be easily restored after solving the Euler–Lagrange equation of motion for the einbein μ which amounts to taking the extremum in the latter. Note that the invariance of the initial action with respect to the change of the proper time,

$$\tau \rightarrow f(\tau), \quad \frac{df}{d\tau} > 0, \quad f(\tau_i) = \tau_i, \quad f(\tau_f) = \tau_f, \quad (2)$$

is preserved if an appropriate rescaling is prescribed to μ :

$$\mu \rightarrow \mu/\dot{f}. \quad (3)$$

The latter invariance means that one deals with a constrained system. For the free particle the only constraint defines the mass shell,

$$p^2 - m^2 = 0, \quad (4)$$

or, in presence of the einbein field μ ,

$$\pi = 0, \quad H = -\frac{p^2 - m^2}{2\mu}, \quad (5)$$

¹In the path integral formalism this transformation is based on the following relation

$$\int D\mu(\tau) \exp\left(-\int d\tau \left(\frac{a\mu}{2} + \frac{b}{2\mu}\right)\right) \sim \exp\left(-\int d\tau \sqrt{ab}\right).$$

²Usually $e = \frac{1}{\mu}$ is referred to as the einbein [7].

with π being the momentum canonically conjugated to μ and H being the Hamiltonian function of the system (in case (4) it identically vanishes). The requirement that the constraint $\pi = 0$ be preserved in time returns one to the mass-shell condition (4):

$$0 = \dot{\pi} = \{\pi H\} = \frac{\partial H}{\partial \mu} = \frac{p^2 - m^2}{2\mu^2} \sim p^2 - m^2. \quad (6)$$

To make things simpler, one can fix the gauge-like freedom (2) identifying the proper time τ with one of the physical coordinates of the particle. The most popular choices are

- the laboratory gauge ($\tau = x_0$);
- the proper time gauge ($\tau = (nx)$, $n_\mu = \frac{P_\mu}{\sqrt{P^2}}$ with P_μ being the total momentum of the system) [10];
- the light-cone gauge ($\tau = \frac{1}{2}(x_0 + x_3) = x_+$),

which lead to quantization of the system on different hypersurfaces.

With the laboratory gauge fixed the Lagrangian function (1) becomes

$$L = -\frac{m^2}{2\mu} - \frac{\mu}{2} + \frac{\mu \dot{\vec{x}}^2}{2}, \quad (7)$$

so that the corresponding Hamiltonian function reads

$$H = \frac{\vec{p}^2 + m^2}{2\mu} + \frac{\mu}{2}, \quad (8)$$

and after taking the extremum in μ one ends with the standard relativistic expression

$$H = \sqrt{\vec{p}^2 + m^2}. \quad (9)$$

B. Einbeins as variational parameters

In the simple example considered above neither the Lagrange nor the Hamilton functions of the system contained $\dot{\mu}$, which allowed one to get rid of μ at any stage by taking the extremum in the latter. It is not so for more complicated systems when a change of variables

is to be performed which touches upon the einbeins. The velocity corresponding to the original degrees of freedom of the system may mix in a very tangled way with those for einbeins, so that it is not a simple task anymore to follow the lines *à la* Dirac [11] to resolve the set of constraints and to get rid of nonphysical degrees of freedom. See, *e.g.*, [6,8,12] for several examples when such a resolution can be done explicitly.

Luckily another approach to einbeins is known [2,13]. They can be treated as variational parameters. Thus one replaces the dynamical function of time $\mu(\tau)$ by the parameter μ_0 independent of τ . The eigenstate problem is solved then, keeping μ_0 constant, so that one has the spectrum $M_{\{n\}}(\mu_0)$, where $\{n\}$ denotes the full set of quantum numbers. Then one is to minimize each eigenenergy independently with respect to μ_0 ³:

$$\left. \frac{\partial M_{\{n\}}(\mu_0)}{\partial \mu_0} \right|_{\mu_0=\mu_0^*} = 0, \quad M_{\{n\}} = M_{\{n\}}(\mu_0^*). \quad (10)$$

Such an approach has a number of advantages. First, it allows one to avoid the tedious algebra of commuting constraints with one another following the standard Dirac technique [11]. Second, it allows one a very simple and physically transparent interpretation of einbeins. Indeed, in formulae (1) and (7) the einbein μ can be treated as an effective mass of the particle; the dynamics of the system remains essentially relativistic, though being non-relativistic in form. If m is the current quark mass, then μ can be viewed as its constituent mass celebrated in hadronic phenomenology. What is more, the current mass can be even put to zero, whereas the Lagrangian approach remains valid in the presence of the einbeins and the standard Hamiltonian technique can be developed then. The latter observation is intensively used in analytic QCD calculations for glue describing gluonic degrees of freedom in glueballs and hybrids [14,15].

³Note that solutions for μ_0 of both signs appear, but only one of them ($\mu_0 > 0$) is finally left. Neglecting the negative solution is the general lack of the einbein field approach and this leads to the fact that quark Zitterbewegung is not taken into account (see also the discussion in Subsection IIID).

An obvious disadvantage of the variational approach to the einbein fields is some loss of accuracy. As a variational method it provides only an approximate solution, giving no hint as to how to estimate the ultimate accuracy of the results. Thus in the next section we test this method, comparing its predictions with exact solutions of some relativistic equations. We consider the accuracy, found to be about 7% at worst, quite reasonable, which justifies our consequent attack on the light-light and heavy-light mesons spectra using this formalism.

III. TESTING THE METHOD

A. Quasiclassics for the spinless Salpeter equation

We start from the Salpeter equation for the quark-antiquark system with equal masses and restrict ourselves to the zero-angular-momentum case for simplicity:

$$\left(2\sqrt{p_r^2 + m^2} + \sigma r\right) \psi_n = M_n^{(ll)} \psi_n, \quad (11)$$

where the subscript (ll) stands for the light-light system.

The quasiclassical quantization condition looks like

$$\int_0^{r_+} p_r(r) dr = \pi \left(n + \frac{3}{4}\right), \quad n = 0, 1, 2, \dots, \quad r_+ = \frac{M_n^{(ll)} - 2m}{\sigma}, \quad (12)$$

where the integral on the l.h.s. can be worked out analytically, yielding

$$M_n^{(ll)} \sqrt{\left(M_n^{(ll)}\right)^2 - 4m^2} - 4m^2 \ln \frac{\sqrt{\left(M_n^{(ll)}\right)^2 - 4m^2} + M_n^{(ll)}}{2m} = 4\sigma\pi \left(n + \frac{3}{4}\right), \quad (13)$$

or approximately ($m \ll \sqrt{\sigma}$) one has

$$\left(M^{(ll)}\right)^2 = 4\pi\sigma \left(n + \frac{3}{4}\right) + 2m^2 \ln \frac{\pi\sigma(n + 3/4)}{m^2} + \dots \quad (14)$$

Solution (14) becomes exact in the limit $m = 0$, whereas for a nonzero mass the leading correction to the linear regime $(M^{(ll)})^2 \sim n$ behaves like

$$\frac{\Delta M_n^2}{M_n^2} = O\left(\frac{m^2}{M_n^2} \ln \frac{M_n}{m}\right) \underset{n \gg 1}{\sim} \frac{\ln n}{n}. \quad (15)$$

For a heavy-light system one has the Salpeter equation

$$\left(\sqrt{p_r^2 + m^2} + \sigma r\right)\psi_n = M_n^{(hl)}\psi_n, \quad (16)$$

where $M_n^{(hl)}$ denotes the excess over the heavy particle mass M . Similarly to (13) one finds then

$$M_n^{(hl)}\sqrt{\left(M_n^{(hl)}\right)^2 - m^2} - m^2 \ln \frac{\sqrt{\left(M_n^{(hl)}\right)^2 - m^2} + M_n^{(hl)}}{m} = 2\sigma\pi\left(n + \frac{3}{4}\right), \quad (17)$$

and formula (15) holds true in this case as well.

Comparing the results of the WKB method with the exact solutions of equation (11) (rows $M_n(\text{WKB})$ and $M_n(\text{exact})$ in Table I), one can see that the error does not exceed 3-4% even for the ground state. See also [16] where the WKB method is tested for light-light mesons.

B. Quasiclassics for the one-particle Dirac equation

As a next example we discuss the one-particle Dirac equation with linearly rising confining potential [17]:

$$(\vec{\alpha}\vec{p} + \beta(m + U) + V)\psi_n = \varepsilon_n\psi_n. \quad (18)$$

The WKB method applied to this equation gives [18,19]

$$\int_{r_-}^{r_+} \left(p + \frac{\kappa w}{pr}\right) dr = \pi\left(n + \frac{1}{2}\right), \quad n = 0, 1, 2, \dots, \quad (19)$$

where

$$\begin{aligned} p &= \sqrt{(\varepsilon - V)^2 - \frac{\kappa^2}{r^2} - (m + U)^2}, \\ w &= -\frac{1}{2r} - \frac{1}{2} \frac{U' - V'}{m + U + \varepsilon - V}, \\ |\kappa| &= j + \frac{1}{2}. \end{aligned} \quad (20)$$

For the most interesting case of purely scalar confinement ($V = 0$, $U = \sigma r$) an approximate quasiclassical solution was found in [19] ($m = 0$):

$$\varepsilon_n^2 = 2\sigma \left(2n + j + \frac{3}{2} + \frac{\text{sgn}\kappa}{2} + \frac{\kappa\sigma}{\pi\varepsilon_n^2} \left(0.38 + \ln \frac{\varepsilon_n^2}{\sigma|\kappa|} \right) + O \left(\left(\frac{\kappa\sigma}{\varepsilon_n^2} \right)^2 \right) \right). \quad (21)$$

A detailed comparison of the results of the WKB method and those following from the recursive formula (21) with exact numerical solutions to equation (18) is given in [20]. Here we only note that the coincidence of the three numbers is impressive as even for the lowest states the discrepancy does not exceed 1%.

C. Quasiclassical variational einbein field (combined) method for the spinless Salpeter equation

Finally we combine the two methods discussed above and apply the WKB approximation to the Hamiltonian of a relativistic system with einbeins introduced as variational parameters. Then the resulting quasiclassical spectrum is minimized with respect to the einbeins. Thus we have a powerful method of solving the eigenvalues problem for various relativistic systems which we call “combined.” Let us test the accuracy of this method first.

We start from the Salpeter equation (11) for the light-light system and introduce the parameter μ_0 as described in Section II:

$$H_1 = 2\sqrt{p_r^2 + m^2} + \sigma r \longrightarrow H_2 = \frac{p_r^2 + m^2}{\mu_0} + \mu_0 + \sigma r. \quad (22)$$

In what follows we consider the massless case substituting $m = 0$ into (22).

We give the analytic formulae for the spectrum of the Salpeter equation (11) obtained using the quasiclassical approximation for the Hamiltonian H_1 (following from equation (13) for $m = 0$), the exact solution for the Hamiltonian H_2 minimized with respect to the einbein field and the result of the combined method when the Bohr-Sommerfeld quantization condition is applied to the Hamiltonian H_2 and the ultimate spectrum is also minimized with respect to μ_0 .

$$M_n^2(\text{WKB}) = 4\pi\sigma \left(n + \frac{3}{4} \right), \quad (23)$$

$$M_n^2(\text{einbein}) = 16\sigma \left(\frac{-\zeta_{n+1}}{3} \right)^{3/2}, \quad (24)$$

$$M_n^2(\text{combined}) = \frac{8\pi}{\sqrt{3}}\sigma \left(n + \frac{3}{4} \right), \quad (25)$$

where ζ_{n+1} is the $(n+1)$ th zero of the Airy function $Ai(z)$ and counting of zeros starts from unity. The extremal values of the einbein field in the latter two cases read

$$\mu_0^*(\text{einbein}) = \sqrt{\sigma} \left(\frac{-\zeta_{n+1}}{3} \right)^{3/4}, \quad \mu_0^*(\text{combined}) = \sqrt{\frac{\sigma(n + 3/4)}{2\sqrt{3}}}, \quad (26)$$

i.e., the effective quark mass is $\mu_0^* \sim \sqrt{\sigma}$ and it appears entirely due to the interquark interaction.

In Table I we compare the results of the above three approximate methods of solving the eigenvalues problem for equation (11) with the exact solution. In the last row we give the accuracy of the combined method *vs* the exact solution. Two conclusions can be deduced from Table I. The first one is that the accuracy of all approximate methods is high enough, including the combined method, which is of most interest for us in view of its consequent applications to the QCD string with quarks at the ends. The other conclusion is that the variational einbein field method gives a systematic overestimation for the excited states which is of order 5-7%.

D. Discussion

Here we would like to make a couple of concluding comments concerning the numerical methods tested in this section, their accuracy and possible ways of their improvement. As stated above the combined quasiclassical variational method is of most interest for us, so we shall concentrate basically on it. The following two remarks are in order here.

From Table I one can see that the relative error is practically constant, tending to the value of 7% for large n . The reason for such a behaviour will become clear if one

compares formulae (23) and (25). Both relations reproduce the same dependence on the radial quantum number n , whereas the difference comes from different slopes, $4\pi\sigma$ in (23) vs $\frac{8\pi}{\sqrt{3}}\sigma$ in (25). Then for highly excited states the error is practically independent of n and can be estimated as

$$\delta = \frac{M_n(\text{combined}) - M_n(\text{exact})}{M_n(\text{combined})} \approx \frac{M_n(\text{combined}) - M_n(\text{WKB})}{M_n(\text{combined})} = 1 - \sqrt{\frac{\sqrt{3}}{2}} \approx 0.07; \quad (27)$$

i.e., the ultimate accuracy of the quasiclassical variational einbein field method (combined method) appears to be about 7%. Introducing, say, a correcting factor in (25) one could overcome the systematic overestimation and reproduce the spectrum with a better accuracy. We shall return to this observation later on when discussing the spectrum of the heavy-light mesons.

Another source of error in the einbein field approach is neglecting the quark Zitterbewegung (see the footnote on page 6). As stated above we neglect the negative sign solution for the einbein field μ_0 expecting its small influence on the spectrum. Let us give some reasoning to justify this action.

It was demonstrated numerically in [21] that the contribution of the quark Z-graphs into M^2 is nearly constant for large excitation numbers and is of order 10%, so that the corresponding shift of M behaves like

$$\Delta M \sim \frac{\Delta M^2}{M} \underset{n \gg 1}{\sim} \frac{1}{\sqrt{n}}, \quad (28)$$

so it is somewhat suppressed.

Besides, the good agreement of our numerical results with those provided by the lattice data and taken from the Particle Data Group can also serve as an *a posteriori* justification of such a neglect. Still some improvements for the einbein field approach are needed to take this effect into account.

IV. REGGE TRAJECTORIES FOR RELATIVISTIC EQUATIONS WITH LOCAL POTENTIALS

It was observed long ago that the mesonic Regge trajectories are almost linear if the total momentum or the radial quantum number is plotted *vs* the mesonic mass squared [22]:

$$M^2(n, J) = c_n n + c_J J + \Delta M^2, \quad (29)$$

where c_n and c_J are the (inverse) slopes while ΔM^2 denotes corrections to the leading linear regime which come from the self-energy, spin splittings, *etc.*

Relations like (29) naturally appear in most of models for confinement, though the (inverse) slopes c_n and c_J are different for different models.

For example the Salpeter equation for the heavy-light system,

$$\left(\sqrt{p_r^2 + p_{\theta,\varphi}^2} + m^2 + \sigma r\right) \psi_{nl} = M_{nl} \psi_{nl}, \quad (30)$$

gives

$$c_J^{(hl)}(Salpeter) = 4\sigma, \quad c_n^{(hl)}(Salpeter) = 2\sigma, \quad (31)$$

where the total momentum J coincides with the orbital one l .

For the light-light system one easily finds, from (31) by a trivial parameters rescaling,

$$c_J^{(ll)}(Salpeter) = 8\sigma, \quad c_n^{(ll)}(Salpeter) = 4\sigma. \quad (32)$$

The one-particle Dirac equation (18) yields different slopes for different natures of the confining force. Thus for the purely vector confinement (potential added to the energy term⁴) one finds

$$c_{J \text{ vec}}^{(hl)}(Dirac) = 4\sigma, \quad (33)$$

whereas, for purely scalar confinement (potential added to the mass term),

⁴We disregard the problem of the Klein paradox here.

$$c_J^{(hl)}(Dirac) = 2\sigma. \quad (34)$$

In the meantime the spectrum (29) is expected to follow from a string-like picture of confinement which predicts the (inverse) Regge slopes to be

$$c_J^{(ll)}(string) = 2\pi\sigma, \quad c_J^{(hl)}(string) = \pi\sigma. \quad (35)$$

One can easily see that none of the relativistic equations considered before gives the correct result (35); moreover the discrepancies are rather large (of order 25%). See also [23] for a discussion of various models of confinement and the corresponding Regge trajectory slopes.

The reason why relativistic Salpeter and Dirac equations fail to reproduce the correct string slope of the Regge trajectories is obvious and quite physically transparent. Indeed, all relativistic equations with local potentials have only a trivial dependence of the interquark interaction on the angular momentum which comes entirely from the quark kinetic energy. Meanwhile, QCD is believed to lead to a string-type interaction between the colour constituents inside hadrons, whereas the QCD string developed between quarks possesses its own inertia and thus it should also contribute to the J -dependent part of the interaction. It is this extra purely string-type piece of the interquark interaction to give an extra contribution to the Regge trajectory slope and to bring it into the correct form of (35). This statement is proved explicitly in the next section, whereas the string dynamics footprint in the heavy-light mesons spectrum is discussed in detail in Section VII.

V. HAMILTONIAN OF THE $Q\bar{Q}$ MESON

A. Quark-antiquark Green's function

We start from the Euclidean Green's function of the $q\bar{q}$ pair in the confining vacuum

$$G_{q\bar{q}} = \langle \Psi_{q\bar{q}}^{(f)}(\bar{x}, \bar{y}|A)^+ \Psi_{q\bar{q}}^{(i)}(x, y|A) \rangle_{q\bar{q}A}, \quad (36)$$

where the initial and the final mesonic wave functions

$$\Psi_{q\bar{q}}^{(i,f)}(x, y|A) = \bar{\Psi}_{\bar{q}}(x)\Phi(x, y)\Gamma^{(i,f)}\Psi_q(y) \quad (37)$$

are gauge invariant due to the standard path-ordered parallel transporter

$$\Phi(x, y) = P \exp \left(ig \int_y^x dz_\mu A_\mu \right), \quad (38)$$

$\Gamma^{(i,f)}$ denote the matrices which might be inserted into the initial and final meson-quark-antiquark vertices.

Integrating out the quark fields in (36), one finds, for the mesonic Green's function,

$$G_{q\bar{q}} = \langle Tr \Gamma^{(f)} S_q(\bar{x}, x|A) \Phi(x, y) \Gamma^{(i)} S_{\bar{q}}(y, \bar{y}|A) \Phi(\bar{y}, \bar{x}) \rangle_A, \quad (39)$$

where the trace stands for both colour and spinor indices. We have neglected here the $1/N_C$ -suppressed quark determinant, describing sea quark pairs.

To proceed further we employ the Feynman-Schwinger representation for the one-fermion propagators in the external field, fix the laboratory gauge for both particles,

$$x_{10} = t_1, \quad x_{20} = t_2, \quad (40)$$

and introduce the einbein fields μ_1 and μ_2 by means of the following change of variables (see [24,2] for details):

$$\mu_i(t_i) = \frac{T}{2s_i} \dot{x}_{i0}(t_i), \quad ds_i D x_{i0} \rightarrow D \mu_i(t_i), \quad i = 1, 2, \quad (41)$$

where $s_{1,2}$ are the Schwinger times, $T = \frac{1}{2}(x_0 + \bar{x}_0 - y_0 - \bar{y}_0)$.

Then the resulting expression for the mesonic Green's function reads [24]

$$G_{q\bar{q}} = \int D\mu_1(t_1) D\mu_2(t_2) D\vec{x}_1 D\vec{x}_2 e^{-K_1 - K_2} Tr \left[\Gamma^{(f)}(m_1 - \hat{D}) \Gamma^{(i)}(m_2 - \hat{D}) \times \right. \quad (42)$$

$$\left. P_\sigma \exp \left(\int_0^T \frac{dt_1}{2\mu_1(t_1)} \sigma_{\mu\nu}^{(1)} \frac{\delta}{i\delta s_{\mu\nu}(x_1(t_1))} \right) \exp \left(- \int_0^T \frac{dt_2}{2\mu_2(t_2)} \sigma_{\mu\nu}^{(2)} \frac{\delta}{i\delta s_{\mu\nu}(x_2(t_2))} \right) \exp(-\sigma S_{\min}) \right],$$

with K_i being the kinetic energies of the quarks

$$K_i = \int_0^T dt_i \left(\frac{m_i^2}{2\mu_i} + \frac{\mu_i}{2} + \frac{\mu_i \dot{x}_i^2}{2} \right), \quad i = 1, 2, \quad (43)$$

$\sigma_{\mu\nu} = \frac{1}{4i}(\gamma_\mu\gamma_\nu - \gamma_\nu\gamma_\mu)$, and $\delta/\delta s_{\mu\nu}$ denotes the derivative with respect to the element of the area S . We have also used the minimal area law asymptotic for an isolated Wilson loop,

$$\left\langle \text{Tr} P \exp \left(ig \oint_C dz_\mu A_\mu \right) \right\rangle_A \sim \exp(-\sigma S_{\min}), \quad (44)$$

which is usually assumed for the stochastic QCD vacuum (see, *e.g.*, [25]) and found on the lattice. Here S_{\min} is the area of the minimal surface swept by the quark and antiquark trajectories.

Looking at (42) one can easily recognize the following three main ingredients: the contribution of the quark, the one of the antiquark, and finally the confining interaction given by the string with tension σ . One can write, for the latter,

$$S_{\min} = \int_0^T dt \int_0^1 d\beta \sqrt{(\dot{w}w')^2 - \dot{w}^2 w'^2}, \quad (45)$$

with $w_\mu(t, \beta)$ being the string profile function chosen in linear form,

$$w_\mu(t, \beta) = \beta x_{1\mu}(t) + (1 - \beta)x_{2\mu}, \quad (46)$$

thus describing the straight-line string which is a reasonable approximation for the minimal surface [2].

Finally, synchronizing the quark and the antiquark times ($t_1 = t_2 = t$) one finds from (42) that in the spinless approximation the quark-antiquark meson can be described by the Lagrangian

$$L(t) = -\frac{m_1^2}{2\mu_1} - \frac{m_2^2}{2\mu_2} - \frac{\mu_1 + \mu_2}{2} + \frac{\mu_1 \dot{\vec{x}}_1^2}{2} + \frac{\mu_2 \dot{\vec{x}}_2^2}{2} - \sigma r \int_0^1 d\beta \sqrt{1 - [\vec{n} \times (\beta \dot{\vec{x}}_1 + (1 - \beta)\dot{\vec{x}}_2)]^2}, \quad (47)$$

where $\vec{r} = \vec{x}_1 - \vec{x}_2$ and $\vec{n} = \vec{r}/r$. Expansion of the surface-ordered exponents in (42) gives a set of spin-dependent corrections to the leading regime (47).

B. Hamiltonian for spinless quarks

Starting from the Lagrangian (47) and introducing an extra einbein field $\nu(t, \beta)$ continuously depending on the internal string coordinate β one can get rid of the square root in

(47) arriving at the Hamiltonian of the $q\bar{q}$ system in the centre-of-mass frame in the form [2]

$$H = \sum_{i=1}^2 \left(\frac{p_r^2 + m_i^2}{2\mu_i} + \frac{\mu_i}{2} \right) + \int_0^1 d\beta \left(\frac{\sigma^2 r^2}{2\nu} + \frac{\nu}{2} \right) + \frac{\vec{L}^2}{2r^2[\mu_1(1-\zeta)^2 + \mu_2\zeta^2 + \int_0^1 d\beta \nu(\beta - \zeta)^2]},$$

$$\zeta = \frac{\mu_1 + \int_0^1 d\beta \nu \beta}{\mu_1 + \mu_2 + \int_0^1 d\beta \nu}. \quad (48)$$

Similarly to μ 's which have the meaning of the constituent quark masses, the einbein ν can be viewed as the density of the string energy. In the simplest case of $l = 0$ one easily finds, for the extremal value of ν ,

$$\nu_0 = \sigma r; \quad (49)$$

i.e., the energy distribution is uniform and the resulting interquark interaction is just the linearly rising potential σr . In the meantime, if $l \neq 0$, then the two contributions can be identified in the last l -dependent term in (48). Roughly speaking the first two μ -dependent terms in the denominator come from the quark kinetic energy. The last term containing the integral over β is nothing but the extra inertia of the string discussed before. Rotating string also contributes to the interquark interaction making it essentially nonlocal, so that the very notion of the interquark potential is not applicable to the system anymore.

Note that the Hamiltonian (48) has the form of sum of the “kinetic” and the “potential” parts, but this is somewhat misleading, as extrema in all three einbeins are understood, so that the ultimate form of the Hamiltonian would be extremely complicated and hardly available for further analytical studies.

Expression (48) can be simplified if one expands the Hamiltonian in powers of $\sqrt{\sigma}/\mu$. One finds then [2,3]

$$H = H_0 + V_{string}, \quad (50)$$

$$H_0 = \sum_{i=1}^2 \left(\frac{\vec{p}^2 + m_i^2}{2\mu_i} + \frac{\mu_i}{2} \right) + \sigma r, \quad (51)$$

$$V_{string} \approx -\frac{\sigma(\mu_1^2 + \mu_2^2 - \mu_1\mu_2)}{6\mu_1^2\mu_2^2} \frac{\vec{L}^2}{r}, \quad (52)$$

where V_{string} is known as the string correction [1,2] and this is the term totally missing in the relativistic equations with local potentials. Indeed, the Salpeter equation with the linearly rising potential is readily reproduced from (51) if extrema in $\mu_{1,2}$ are taken explicitly, whereas the string correction is lost. Meanwhile, its sign is negative so that the contribution of the string lowers the energy of the system, thus giving a negative contribution to the masses of orbitally excited states, leaving those with $l = 0$ intact. In Section VI we shall demonstrate how a proper account of the string dynamics in the full Hamiltonian (48) brings the Regge trajectory slope to the correct value (35), whereas in Section VII the string correction (52) will be demonstrated to solve the problem of the identification of the resonance $D(2637)$ recently claimed by the DELPHI Collaboration [4,5].

C. Spin-dependent corrections

Let us return to the quark-antiquark Green's function (42) and extract the nonperturbative spin-orbit interaction. Following [26,27] one finds

$$V_{so}^{np} = -\frac{\sigma}{2r} \left(\frac{\vec{S}_1 \vec{L}}{\mu_1^2} + \frac{\vec{S}_2 \vec{L}}{\mu_2^2} \right). \quad (53)$$

It follows from [26,27] that all potentials $V_i(r)$ (in the notation of [28]) contain both perturbative and nonperturbative pieces given there in explicit form. One can argue that at large distances only the piece (53) is left whereas for light quarks all nonperturbative ones may be important (see [29]).

Now, to have a full picture of the interquark interaction one is to supply the purely non-perturbative string-type interaction described by the Hamiltonian (48) by the perturbative gluon exchange adding the colour Coulomb potential to the Hamiltonian H_0 from (51) and calculating the corresponding spin-dependent perturbative terms in addition to the potential (53). The result reads

$$H_0 = \sum_{i=1}^2 \left(\frac{\vec{p}^2 + m_i^2}{2\mu_i} + \frac{\mu_i}{2} \right) + \sigma r - \frac{4}{3} \frac{\alpha_s}{r} - C_0, \quad (54)$$

where we have also added the overall constant shift C_0 and

$$\begin{aligned} V_{sd} = & \frac{8\pi\kappa}{3\mu_1\mu_2} (\vec{S}_1\vec{S}_2) |\psi(0)|^2 - \frac{\sigma}{2r} \left(\frac{\vec{S}_1\vec{L}}{\mu_1^2} + \frac{\vec{S}_2\vec{L}}{\mu_2^2} \right) + \frac{\kappa}{r^3} \left(\frac{1}{2\mu_1} + \frac{1}{\mu_2} \right) \frac{\vec{S}_1\vec{L}}{\mu_1} + \frac{\kappa}{r^3} \left(\frac{1}{2\mu_2} + \frac{1}{\mu_1} \right) \frac{\vec{S}_2\vec{L}}{\mu_2} \\ & + \frac{\kappa}{\mu_1\mu_2 r^3} \left(3(\vec{S}_1\vec{n})(\vec{S}_2\vec{n}) - (\vec{S}_1\vec{S}_2) \right) + \frac{\kappa^2}{2\pi\mu^2 r^3} (\vec{S}\vec{L}) (2 - \ln(\mu r) - \gamma_E), \quad \gamma_E = 0.57, \end{aligned} \quad (55)$$

with $\kappa = \frac{4}{3}\alpha_s$, $\mu = \frac{\mu_1\mu_2}{\mu_1+\mu_2}$. We have also added the term of order α_s^2 which comes from one-loop calculations and is intensively discussed in the literature [30,31,29]. It is important to stress that C_0 is due to the nonperturbative self-energy of light quarks, which explains the later numerical inputs.

An important comment concerning the expansion (55) is in order. Up to the last term the expression (55) coincides in form with the Eichten–Feiberg–Gromes result [28], but we have effective quark masses μ_i in the denominators instead of the current ones m_i . Once $\mu_i \sim \sqrt{\langle \vec{p}^2 \rangle + m_i^2} > m_i$ or even $\mu_i \gg m_i$, then the result (55) is applicable to the case of light quark flavours, when the expansion of the interaction in the inverse powers of the quark mass m_i obviously fails. The values of μ 's are defined dynamically and differ from state to state (see [26] for details).

The Hamiltonian (54) with spin-dependent terms (55) will be used for explicit calculations for heavy-light mesons. In the case of light-light states one should include additional nonperturbative spin-dependent terms (see [26] and references therein). The masses of light-light mesons listed in Table II have been calculated from the Regge trajectories which do not take into account spin-dependent terms and we give them for the sake of comparison. A more detailed calculation for the light mesons taking these effects into account can be found in [29].

VI. SPECTRUM OF LIGHT-LIGHT MESONS

A. Angular-momentum-dependent potential and Regge trajectories

Starting from the Hamiltonian (48) we stick with the case of equal quark masses m

$$H = \frac{p_r^2 + m^2}{\mu} + \mu + \frac{\vec{L}^2/r^2}{\mu + 2 \int_0^1 (\beta - \frac{1}{2})^2 \nu d\beta} + \frac{\sigma^2 r^2}{2} \int_0^1 \frac{d\beta}{\nu} + \int_0^1 \frac{\nu}{2} d\beta. \quad (56)$$

The extremal value of the einbein field ν can be found explicitly and reads [20]

$$\nu_0(\beta) = \frac{\sigma r}{\sqrt{1 - 4y^2(\beta - \frac{1}{2})^2}}, \quad (57)$$

where y is the solution of the transcendental equation

$$\frac{L}{\sigma r^2} = \frac{1}{4y^2} (\arcsin y - y\sqrt{1 - y^2}) + \frac{\mu y}{\sigma r}, \quad (58)$$

and $\vec{L}^2 = l(l + 1)$.

For large angular momenta the contribution of the quarks (the last term on the r.h.s. of (58)) is negligible so that the maximal possible value $y = 1$ is reached, thus yielding the solution for the free open string [2] (see also the second entry in [12]).

With the extremal value ν_0 from (57) inserted, the Hamiltonian (56) takes the form

$$H = \frac{p_r^2 + m^2}{\mu(\tau)} + \mu(\tau) + \frac{\sigma r}{y} \arcsin y + \mu(\tau)y^2, \quad (59)$$

with y defined by equation (58). The last two terms on the r.h.s. of equation (59) can be considered as an effective “potential”

$$U(\mu, r) = \frac{\sigma r}{y} \arcsin y + \mu(\tau)y^2, \quad (60)$$

which is nontrivially l dependent. In Fig.1 we give the form of the effective potential (60) for a couple of low-lying states (solid line). It has the same asymptotic as the naive sum of the linearly rising potential and the centrifugal barrier coming from the kinetic energy of the quarks (dotted line). In the meantime it differs from the latter at finite distances. The only exception is the case of zero angular momentum which should be treated separately and leads to the linearly rising potential for any interquark separation.

B. Numerical results

Following the variational einbein field method described and tested above, we start from the Hamiltonian (59) and change the einbein field μ for the variational parameter μ_0 [20], so that one has

$$H = \frac{p_r^2 + m^2}{\mu_0} + \mu_0 + U(\mu_0, r), \quad (61)$$

$$U(\mu_0, r) = \frac{\sigma r}{y} \arcsin y + \mu_0 y^2. \quad (62)$$

Then the quasiclassical method applied to the Hamiltonian (61) gives

$$\int_{r_-}^{r_+} p_r(r) dr = \pi \left(n + \frac{1}{2} \right), \quad (63)$$

with

$$p_r(r) = \sqrt{\mu_0(M - \mu_0 - U(\mu_0, r)) - m^2}. \quad (64)$$

The eigenvalues $M_{nl}(\mu_0)$ for $m = 0$ were found numerically from (63), (64) and the minimization procedure with respect to μ_0 was used then. Results for M_{nl} are given in Table II and depicted in Fig.2 demonstrating very nearly straight lines with approximately string slope $(2\pi\sigma)^{-1}$ in l and twice as small slope in n . Note that it is the region of intermediate values of r that plays the crucial role in the Bohr-Sommerfeld integral (63), *i.e.*, the region where the nontrivial dependence of the effective potential $U(\mu_0, r)$ on the angular momentum is most important (see Fig.1).

In Table III we give a comparison of the masses of several light-light mesonic states extracted by means of the numerical results from Table II with the experimental data and theoretical predictions taken from [32]. We have fitted our results to the experimental spectrum using the negative constant ΔM^2 (see equation (29)).

C. Discussion

Let us recall the results obtained for the light-light mesons and discuss problems connected to the given approach. The net result of the current section is the l -dependent effective interquark potential which gives the naive linearly rising interaction only for $l = 0$. It was observed long ago [33,2] that for large angular momenta the quark dynamics is negligible and the slope (35) naturally appears from the picture of open rotating string. In the present paper we find that for massless quarks even the low-lying mesonic states demonstrate nearly straight-line Regge trajectories with string slope (35).

One problem clearly seen from Figs.2,3 is the leading trajectory intercept $l_0 \equiv l$ ($M^2 = 0$). To reproduce the experimental intercept around -0.5 (see Fig.3) starting from the theoretical one +0.5 (see left plot in Fig.2) one needs a large negative constant added either to the Hamiltonian (48) (see, *e.g.*, C_0 in equation (54)) or in the form of ΔM^2 directly in (29) (see also Table III). Once the first way might violate the linearity of the Regge trajectories, then one should expect QCD to prefer the second one, though the first way remains more attractive from the practical point of view and will be used in calculations of the heavy-light mesons spectrum in the next section.

Another problem is that one of the most intriguing questions of mesonic spectroscopy, the π - ρ splitting (and a similar problem in the strange sector) cannot be addressed in our model. Taking the exact solution of the spinless Salpeter equation (11) with $n = l = 0$ (see Table I with an appropriate rescaling from $\sigma = 0.2\text{GeV}^2$ to $\sigma = 0.17\text{GeV}^2$) one finds for the ρ mass squared the value of order 1.7GeV^2 which does not violate the linearity of the trajectory (see the circled dot in Fig.2). If the overall negative shift with $\sqrt{|\Delta M^2|} = 1126\text{MeV}^2$ (see Table III) is applied to this state, then one arrives at a ρ -meson mass about 775MeV , *i.e.*, a value very close to the experimental one. Note that we have practically coinciding constants for the ρ - and a -meson trajectories (see the caption for Table III), which supports the idea that ΔM^2 can be associated with quark self-energies.

Meanwhile, one cannot pretend to describe pions (kaons) in the same framework as their

Goldstone nature is not implemented in the current model. In realistic quantum-field-theory-based models each mesonic state possesses two wave functions which describe the motion forward and backward in time of the $q\bar{q}$ pair inside the meson [34]. The backward motion is suppressed if at least one of the quarks is heavy, for highly excited states and in the infinite-momentum frame. For the chiral pion, which is expected to be strictly massless in the chiral limit, the two wave functions are of the same order of magnitude (see, *e.g.*, [35] for an explicit pionic solution in QCD₂), so that none of them can be neglected. This explains why the naive estimate for the pion mass lies much higher than the experimentally observed value of 140MeV . For the first excited state, ρ meson, this effect is already suppressed, though one still has to be careful to neglect the backward motion of the quarks. The progress in this direction was achieved in recent papers by one of the authors (Yu.S.) [19], where a Dirac-type equation was derived for the heavy-light system and the properties of its solutions were investigated. This new formalism is expected to allow consideration of pionic Regge trajectories as it has the chiral symmetry breaking built in.

VII. SPECTRUM OF HEAVY-LIGHT MESONS

All results obtained for the light-light mesons in Section VI can be reproduced for the heavy-light states, so that in the one-body limit the Regge trajectories with the correct string (inverse) slope $\pi\sigma$ are readily reproduced. Meanwhile, the aim of this study is to take into account corrections to the leading regime which come from the spin-dependent terms in the interquark interaction as well as those due to the finiteness of the heavy quark mass. Corrections of both types are important for establishing the correct spectra of D and B mesons which are the main target of the present investigation.

A. Spectrum of the spinless heavy-light system

In this subsection we study the spectrum of the heavy-light mesons, disregarding the quark spins. This amounts to solving the Schrödinger-like equation for the Hamiltonian H_0

from (54). Note that to this end one needs to know the nonrelativistic spectrum in the potential which is the sum of the linearly rising and Coulomb parts [26,36,3]:

$$\left(-\frac{d^2}{d\vec{x}^2} + |\vec{x}| - \frac{\lambda}{|\vec{x}|}\right) \chi_\lambda = a(\lambda) \chi_\lambda, \quad (65)$$

where

$$\lambda = \kappa \left(\frac{2\mu}{\sqrt{\sigma}}\right)^{2/3}, \quad \kappa = \frac{4}{3}\alpha_s, \quad \mu = \frac{\mu_1\mu_2}{\mu_1 + \mu_2}.$$

If solutions of (65) for χ_λ and $a(\lambda)$ are known as functions of the reduced Coulomb potential strength λ , then one can find the following expressions for the extremal values of the einbeins (constituent quark masses):

$$\mu_1(\lambda) = \sqrt{m_1^2 + \Delta^2(\lambda)}, \quad \mu_2(\lambda) = \sqrt{m_2^2 + \Delta^2(\lambda)}, \quad \mu(\lambda) = \frac{1}{2}\sqrt{\sigma} \left(\frac{\lambda}{\kappa}\right)^{3/2}, \quad (66)$$

with $\Delta(\lambda)$ given by

$$\Delta^2(\lambda) = \frac{\sigma\lambda}{3\kappa} \left(a + 2\lambda \left|\frac{\partial a}{\partial \lambda}\right|\right).$$

The definition of the reduced einbein field μ via μ_1 and μ_2 leads to the equation defining λ

$$\mu(\lambda) = \frac{\mu_1(\lambda)\mu_2(\lambda)}{\mu_1(\lambda) + \mu_2(\lambda)}. \quad (67)$$

Technically this means that one should generate self-consistent solutions to equations (65) and (67) which are subject to numerical calculations [36,3]. In Table IV we give such solutions for several radial and orbital excitations in D -, D_s -, B -, and B_s -mesonic spectra. We use the standard values for the string tension, the strong coupling constant, and the current quarks masses. Note that α_s is chosen close to its frozen value [37] and it does not change a lot between D and B mesons. The reason is that in both cases one has a light quark moving in the field of a very heavy one, so that the one-gluon exchange depends on the size of the system, rather than on its total mass. Once the difference in size between D and B mesons is not that large, the difference between the two values of the strong coupling constant is also small (see Table IV).

The ψ function at the origin given in the last column of Table IV and which will be used later on for spin-spin splittings is defined for radially excited states as

$$|\psi(0)|^2 = \frac{2\mu\sigma}{4\pi} \left(1 + \lambda \langle x^{-2} \rangle\right), \quad (68)$$

where

$$\langle r^N \rangle = (2\mu\sigma)^{N/3} \langle x^N \rangle = (2\mu\sigma)^{N/3} \int_0^\infty x^{N+2} |\chi_\lambda(x)|^2 dx, \quad N > -3 - 2l, \quad (69)$$

which immediately follows from the properties of equation (65) and the corresponding re-definition of variables.

B. Spin-spin and spin-orbit splittings. The string correction

In this subsection we calculate the spin-dependent corrections to the results given in Table IV as well as those due to the proper string dynamics and which were intensively discussed before.

The eigenstates of the Hamiltonian H_0 from (54), which we consider to be the zeroth approximation, can be specified in the form of terms $n^{2S+1}L_J$ (n being the radial quantum number) as the angular momentum \vec{L} , the total spin \vec{S} , and the total momentum $\vec{J} = \vec{L} + \vec{S}$ are separately conserved by H_0 . The corresponding matrix elements for various operators present in (55) read as follows:

$$\begin{aligned} &^{2S+1}P_J \\ &\langle {}^1P_1 | \vec{S}_1 \vec{L} | {}^1P_1 \rangle = 0, \quad \langle {}^1P_1 | \vec{S}_2 \vec{L} | {}^1P_1 \rangle = 0, \quad \langle {}^1P_1 | (\vec{S}_1 \vec{n})(\vec{S}_2 \vec{n}) | {}^1P_1 \rangle = -\frac{1}{4}, \\ &\langle {}^3P_0 | \vec{S}_1 \vec{L} | {}^3P_0 \rangle = -1, \quad \langle {}^3P_0 | \vec{S}_2 \vec{L} | {}^3P_0 \rangle = -1, \quad \langle {}^3P_0 | (\vec{S}_1 \vec{n})(\vec{S}_2 \vec{n}) | {}^3P_0 \rangle = -\frac{1}{4}, \\ &\langle {}^3P_1 | \vec{S}_1 \vec{L} | {}^3P_1 \rangle = -\frac{1}{2}, \quad \langle {}^3P_1 | \vec{S}_2 \vec{L} | {}^3P_1 \rangle = -\frac{1}{2}, \quad \langle {}^3P_1 | (\vec{S}_1 \vec{n})(\vec{S}_2 \vec{n}) | {}^3P_1 \rangle = \frac{1}{4}, \\ &\langle {}^3P_2 | \vec{S}_1 \vec{L} | {}^3P_2 \rangle = \frac{1}{2}, \quad \langle {}^3P_2 | \vec{S}_2 \vec{L} | {}^3P_2 \rangle = \frac{1}{2}, \quad \langle {}^3P_2 | (\vec{S}_1 \vec{n})(\vec{S}_2 \vec{n}) | {}^3P_2 \rangle = \frac{1}{20}; \end{aligned} \quad (70)$$

$^{2S+1}D_J$

$$\begin{aligned}
\langle ^1D_2|\vec{S}_1\vec{L}|^1D_2\rangle &= 0, & \langle ^1D_2|\vec{S}_2\vec{L}|^1D_2\rangle &= 0, & \langle ^1D_2|(\vec{S}_1\vec{n})(\vec{S}_2\vec{n})|^1D_2\rangle &= -\frac{1}{4}, \\
\langle ^3D_1|\vec{S}_1\vec{L}|^3D_1\rangle &= -\frac{3}{2}, & \langle ^3D_1|\vec{S}_2\vec{L}|^3D_1\rangle &= -\frac{3}{2}, & \langle ^3D_1|(\vec{S}_1\vec{n})(\vec{S}_2\vec{n})|^3D_1\rangle &= -\frac{1}{12}, \\
\langle ^3D_2|\vec{S}_1\vec{L}|^3D_2\rangle &= -\frac{1}{2}, & \langle ^3D_2|\vec{S}_2\vec{L}|^3D_2\rangle &= -\frac{1}{2}, & \langle ^3D_2|(\vec{S}_1\vec{n})(\vec{S}_2\vec{n})|^3D_2\rangle &= \frac{1}{4}, \\
\langle ^3D_3|\vec{S}_1\vec{L}|^3D_3\rangle &= 1, & \langle ^3D_3|\vec{S}_2\vec{L}|^3D_3\rangle &= 1, & \langle ^3D_3|(\vec{S}_1\vec{n})(\vec{S}_2\vec{n})|^3D_3\rangle &= \frac{1}{28}.
\end{aligned} \tag{71}$$

The interaction V_{sd} given by (55) mixes orbitally excited states with different spins, so that the transition matrix elements are given by

$$\begin{aligned}
\langle ^1P_1|\vec{S}_1\vec{L}|^3P_1\rangle &= \frac{1}{\sqrt{2}}, & \langle ^1P_1|\vec{S}_2\vec{L}|^3P_1\rangle &= -\frac{1}{\sqrt{2}}, \\
\langle ^1D_2|\vec{S}_1\vec{L}|^3D_2\rangle &= \sqrt{\frac{3}{2}}, & \langle ^1D_2|\vec{S}_2\vec{L}|^3D_2\rangle &= -\sqrt{\frac{3}{2}},
\end{aligned} \tag{72}$$

which lead to mixing within $|^1P_1\rangle$, $|^3P_1\rangle$ and $|^1D_2\rangle$, $|^3D_2\rangle$ pairs so that the physical states are subject to matrix equations of the following type:

$$\begin{vmatrix} E_1 - E & V_{12} \\ V_{12}^* & E_2 - E \end{vmatrix} = 0. \tag{73}$$

Another important ingredient is the string correction given by (52) which leads to an extra negative shift for orbitally excited states

$$\delta M_l \approx -\frac{\sigma(\mu_1^2 + \mu_2^2 - \mu_1\mu_2)}{6\mu_1^2\mu_2^2}l(l+1)\langle r^{-1} \rangle. \tag{74}$$

Thus the model is totally fixed and the only remaining fitting parameter is the overall spectrum shift C_0 which finally takes the following values:

$$C_0(D) = 212MeV, \quad C_0(D_s) = 124MeV, \quad C_0(B) = 203MeV, \quad C_0(B_s) = 124MeV. \tag{75}$$

Note that C_0 does not depend on the heavy quark ($C_0(D) \approx C_0(B)$, $C_0(D_s) \approx C_0(B_s)$) and is completely defined by the properties of the light one. For states with two light quarks

one would have an overall negative shift $2C_0$, which gives the contribution $-4C_0(M_n - C_0)$ to M_n^2 . In case of the ρ meson this provides a negative constant of order 1GeV , *i.e.*, the right value needed to bring the theoretical intercept l_0 into the correct experimental one (see $|\Delta M^2|$ in Table III).

C. Comparison with the experimental and lattice data. “Mystery” of the $D(2637)$ state

In Tables V and VI we compare the results of our numerical calculations for the spectrum and splittings with experimental and recent lattice data as well as with the theoretical predictions from [32] and [40]. The underlined figures in Table V are considered as the most probable candidates for the experimentally observed values. One can see good agreement between our theoretical predictions and the experimental values, as well as with the lattice calculations [38,39]. To demonstrate the relevance of the corrections due to the heavy mass we consider a simplified system containing one infinitely heavy particle and the light one having its real mass. The best fits for the experimental spectra with the results for such simplified systems are also given in Table V in the column entitled $M_{hl}^{(0)}$ for comparison. One can easily see that corrections in the inverse powers of the heavy mass are strongly needed to reproduce the experimental spectrum with a reasonable accuracy and to remove degeneracy of S states.

Now we are in the position to resolve the “mystery” of the $D(2637)$ state (and a similar one in the B -meson spectrum). This state was claimed recently by the DELPHI Collaboration [4,5], but once its quantum numbers were not defined, then there was a problem of the identification of this state. In most quark models (see also Table V) the first radial excitation $J^P = 0^-$ lies approximately in the desired region of mass, but estimates of the width of such a state lead to a confusion, as all such estimates give values much larger than the width of about 15MeV reported by DELPHI. The only would-be way out of the problem is to identify this narrow state with orbital excitations with J^P being 2^- or 3^- . In spite

of the fact that orbitally excited states are really narrower than the radially excited ones and can have a width compatible with the experimental value, the following two objections can be made [41]: i) quark models predict orbitally excited mesons to be at least 50MeV heavier than needed, and ii) a neighboring slightly more massive state should be observed as well.

It follows from Table V that we can remove both objections mentioned above (see also [3]). Indeed, one can easily see that orbitally excited states 2^- and 3^- lie even somewhat lower than the radial excitation 0^- . The reason for that is the negative string correction (74) for the orbitally excited states which comes from the proper dynamics of the string. Besides that, the single D -wave 3^- state is an even more probable candidate for the role of the observed $D(2637)$ resonance than the lightest one from the pair of 2^- states, so that the problem of the “missing state” is also avoided.

Note that our predictions $D(2654)$, $D(2663)$, and $D(2664)$ give larger masses compared to the experimental one. This must be a reflection of the general lack of the variational einbein field method (μ technique) discussed before, which gives slightly overestimated values for the spectrum of excited states (see Table I and the discussion in subsection III D).

D. A bridge to the Heavy Quark Effective Theory

In this subsection we discuss the correspondence between our model and the Heavy Quark Effective Theory (HQET) approach widely discussed in the literature (see [42,43] and references therein). We use the standard parametrization for the heavy-light meson mass,

$$M_{hl} = m_Q + \bar{\Lambda} - \frac{1}{2m_Q}(\lambda_1 + d_H \lambda_2) + O\left(\frac{1}{m_Q^2}\right), \quad (76)$$

where m_Q is the mass of the heavy constituent, and the coefficient d_H describes the hyperfine splitting,

$$d_H = \begin{cases} +3, & \text{for } 0^- \text{ states,} \\ -1, & \text{for } 1^- \text{ states,} \end{cases} \quad (77)$$

whereas $\bar{\Lambda}$, λ_1 , and λ_2 are free parameters which are subject to theoretical investigation. The parameter λ_2 is directly connected to the splitting between 1^3S_1 and 1^1S_0 states and can be estimated from the experimental B -mesonic spectrum to be

$$\lambda_2 = \frac{1}{4}(M_{B^*} - M_B) \approx 0.12 \text{GeV}^2. \quad (78)$$

From Table VI one can easily find our prediction for λ_2

$$\lambda_2 \approx 0.16 \text{GeV}^2, \quad (79)$$

which being slightly overestimated is still in reasonable agreement with the experimental value (78).

In the meantime our model allows direct calculation of the parameters $\bar{\Lambda}$, λ_1 , and λ_2 based on the Hamiltonian (54). We apply the variational procedure described above to the idealized system with $m_1 \equiv m_Q \rightarrow \infty$ and $m_2 \rightarrow 0$. This yields

$$\bar{\Lambda} = \sqrt{\sigma} \left[\sqrt{\frac{\kappa}{\lambda_0}} a(\lambda_0) + \sqrt{\frac{\lambda_0}{12\kappa} \left(a(\lambda_0) + 2\lambda_0 \left| \frac{\partial a}{\partial \lambda_0} \right| \right)} \right], \quad (80)$$

where $\kappa = \frac{4}{3}\alpha_s$, and $a(\lambda)$ is the dimensionless eigenvalue introduced in (65) (see subsection VII A); λ_0 is a solution to the equation

$$\lambda^2 = \frac{4}{3}\kappa^2 \left(a + 2\lambda \left| \frac{\partial a}{\partial \lambda} \right| \right). \quad (81)$$

Then one can extract the coefficient λ_2 from the first term in equation (55):

$$\lambda_2 = -\frac{4\pi\kappa}{3\mu_2} |\psi(0)|^2 = -\frac{2}{3}\sigma\kappa \left(1 + \lambda_0 \langle x^{-2} \rangle \right). \quad (82)$$

An analytical formula for λ_1 is also available, but it is rather bulky and we do not give it here. For $\alpha_s = 0.39$ one can find the numerical solution to equation (81) to be $\lambda_0 = 1.175$. The corresponding values for $\bar{\Lambda}$, λ_1 , and λ_2 are given in the first column of Table VII where they are compared with the results of other approaches.

Another way to estimate the discussed constants is to find the best fit of the form

$$M_{fit} = m_Q + \bar{\Lambda} + C_0 - \frac{\lambda_1}{2m_Q}, \quad (83)$$

with $\bar{\Lambda}$ and λ_1 being the fitting parameters and $C_0 = 203MeV$ taken from (75), for eigenvalues of the Hamiltonian (54) with m_Q varied around the bottom quark mass $m_b = 4.8GeV$ (we use the region $4GeV < m_Q < 6GeV$). The coefficient λ_2 can be found using formula (82) with λ_0 changed for the exact solution for λ taken from Table IV. Results are listed in the second column of Table VII.

One can see our figures to be in general agreement with those found in other approaches among which we mention the QCD sum rules method [44], the inclusive semileptonic B -meson decays [45], and the Dyson-Schwinger equation for the system of a light quark and a static antiquark [46]. We find the parameter λ_1 to be rather sensitive to the strong coupling constant α_s . For example, for $\alpha_s = 0.3$ one has $\lambda_1 = -0.38GeV^2$ which should be confronted with the value $\lambda_1 = -0.506GeV^2$ from the first column of Table VII found for $\alpha_s = 0.39$.

All our predictions for λ_2 exceed the value given by equation (78). The reason is the slightly overestimated value of $\psi(0)$ given by the variational einbein field approach.

One should appreciate the advantage of the einbein field method which allows one to obtain relatively simple analytical formulae for various parameters and to investigate their dependence on the strong coupling constant α_s (the dependence on the only dimensional parameter σ is uniquely restored, giving $\bar{\Lambda} \sim \sqrt{\sigma}$ and $\lambda_1 \sim \lambda_2 \sim \sigma$).

VIII. CONCLUSIONS

In conclusion let us briefly recall the main results obtained in the present paper.

We use the model for the QCD string with quarks at the ends to calculate the spectra of light-light and heavy-light mesons. There are two main points in which we differ from other approaches to the same problem based on various relativistic Hamiltonians and equations with local potentials. The first point is that we do not introduce the constituent mass by

hand. On the contrary, starting from the current mass we naturally arrive at the effective quark masses which appear due to the interaction. Moreover, the resulting effective mass is large enough even for the lightest quarks and lowest states in the spectrum, so that the spin-dependent terms in the interquark interaction can be treated as perturbations in most cases (except for pions and kaons) and thus accounted for in this way.

The second advantage of the method is that the dynamics of the QCD string naturally enters the game and it can be studied systematically. A proper account of this dynamics allows one to resolve several problems of the mesonic spectroscopy; namely, one can find that the rotating string lowers the masses of orbitally excited states, bringing the (inverse) slope of Regge trajectories to their correct values ($2\pi\sigma$ for light-light and $\pi\sigma$ for heavy-light states). In addition, this allows one to resolve the problem of the identification of the $D(2637)$ state recently claimed by the DELPHI Collaboration and which is known to lead to a contradiction between its small width, incompatible with the decay modes for the radial excitation, and its mass lying considerably lower than the values predicted by the quark models for orbitally excited states. In the meantime, taking into account the negative string correction contributing into the masses of orbitally excited mesons readily resolves this “mystery” for the $D(2637)$ state as well as for its counterpart in the spectrum of B mesons.

For the heavy-light system we extract the constants $\bar{\Lambda}$, λ_1 , and λ_2 used in the framework of the Heavy Quark Effective Theory, for which we derive analytical formulae. We find our numerical results to be in agreement with those obtained from the experimental data and calculations in other approaches like QCD sum rules, inclusive semileptonic B -meson decays, and the relativistic Dyson-Schwinger equation for the $q\bar{Q}$ system.

We also conclude that the string-like interaction favoured by QCD invalidates the very notion of any local interquark potential, still leaving room to the einbein field method for the Hamiltonian approach to the bound states of quarks and gluons in QCD. Being rather accurate, this method still requires improvements to increase the accuracy and to have the full control over it.

The authors are grateful to A.M.Badalian, P.Bicudo, R.N.Faustov, A.B.Kaidalov, V.S.Popov and E.Ribeiro for useful discussions and valuable comments and to V.L.Morgunov and B.L.G.Bakker for providing numerical solutions to some equations. One of the authors (A.N.) would like to thank the staff of the Centro de Física das Interações Fundamentais (CFIF-IST) for cordial hospitality during his stay in Lisbon.

Financial support of RFFI grants 00-02-17836 and 00-15-96786, INTAS-RFFI grant IR-97-232 and INTAS CALL 2000, project # 110 is gratefully acknowledged. One of the authors (A.N.) is also supported via RFFI grant 01-02-06273.

-
- [1] J.Merlin and J.Paton, J.Phys. **G11** (1985) 439
 - [2] A.Yu.Dubin, A.B.Kaidalov, Yu.A.Simonov, Phys.Lett. **B323** (1994) 41; Phys.Lett. **B343** (1995) 310
 - [3] Yu.S.Kalashnikova and A.V.Nefediev, Phys.Lett. **B492** (2000) 91
 - [4] DELPHI Collaboration, P.Abreu *et.al.*, Phys.Lett. **B426** (1998) 231
 - [5] M.Feindt, O.Podorin (DELPHI Collaboration), contr.pa01-021 ICHEP'96 Warsaw, DELPHI 96-93 CONF 22;
C.Weiser in *Proceedings of the 28th International Conference on High Energy Physics*, edited by Z.Ajduk, A.K.Worblewski, (World Scientific, Singapore 1997), p. 531
 - [6] Yu.S.Kalashnikova and A.V.Nefediev, Yad.Fiz. **60** (1997) 1529 (Phys.Atom.Nucl. **60** (1997) 1389)
 - [7] L.Brink, P.Di Vecchia, P.Howe, Nucl.Phys. **B118** (1977) 76
 - [8] E.S.Fradkin and D.M.Gitman, Phys.Rev. **D44** (1991) 3230;
G.V.Grygoryan and R.P.Grigoryan, Phys.Atom.Nucl. **53** (1991) 1737;
Yu.S.Kalashnikova and A.V.Nefediev, Phys.Atom.Nucl. **62** (1999) 377

- [9] A.M.Polyakov, *Gauge Fields and Strings* (Harwood Academic, Chur, Switzerland, 1987)
- [10] F.Rohrlich, Ann.Phys. **117** (1979) 292;
M.J.King, F.Rohrlich, Ann.Phys. **130** (1980) 350
- [11] P.A.M.Dirac, *Lectures on Quantum Mechanics* (Belter Graduate School of Science, Yeshiva University, New York, 1964)
- [12] Yu.S.Kalashnikova and A.V.Nefediev, Phys.Lett. **B399** (1997) 274; Yad.Fiz. **61** (1998) 871
(Phys.Atom.Nucl. **61** (1998) 785)
- [13] Yu.A.Simonov, Phys.Lett. **B226** (1989) 151
- [14] Yu.A.Simonov, in *Proceedings of Hadron'93*, Como, edited by T.Bressani, A.Felicielo, G.Preparata and P.G.Ratcliffe (Nuovo Cim. **A107** (1994) 2629);
Yu.S.Kalashnikova and Yu.B.Yufryakov, Phys. Lett. **B359** (1995) 175; Yad.Fiz. **60** (1997) 374
(Phys.At.Nucl. **60** (1997) 307)
- [15] Yu.A.Simonov and A.B.Kaidalov, Phys.Lett. **B477** (2000) 163; Phys.At.Nucl. **63** (2000) 1428
- [16] V.D.Mur, B.M.Karnakov and V.S.Popov (in preparation)
- [17] V.D.Mur, V.S.Popov, Yu.A.Simonov and V.P.Yurov, Zh.Eksp.Teor.Fiz. **105** (1994) 3 (JETP **78** (1994) 1)
- [18] M.S.Marinov and V.S.Popov, Zh.Eksp.Teor.Fiz. **67** (1974) 1250;
V.L.Eletsky, V.D.Mur, P.S.Popov and D.N.Voskresensky, Zh.Eksp.Teor.Fiz. **76** (1979) 431
(JETP **49** (1979) 232); Phys.Lett. **B80** (1978) 68
- [19] Yu.A.Simonov, Yad. Fiz. **60** (1997) 2252 (Phys.At.Nucl. **60** (1997) 2069);
Yu.A.Simonov, J.A.Tjon, Phys.Rev. **D62** (2000) 094511
- [20] V.L.Morgunov, A.V.Nefediev and Yu.A.Simonov, Phys.Lett. **B459** (1999) 653
- [21] V.L. Morgunov, V.I. Shevchenko, Yu.A. Simonov, Yad.Fiz. **61** (1998) 739 (Phys.Atom.Nucl.

61 (1998) 664)

- [22] G.F.Chew, Rev.Mod.Phys. **34** (1962) 394;
I.Yu.Kobzarev, B.V. Martemyanov, M.G.Schepkin, Usp.Fiz.Nauk **162** (1992) 1 (Sov.Phys.Usp. **162** (1992) 1);
M.G.Olsson Phys.Rev.**D55** (1997) 5479;
B.M.Barbashov and V.V.Nesterenko, *Relativistic String Model in Hadron Physics* (Energoatomizdat, Moscow, 1987)
- [23] T.J.Allen, M.G.Olsson, S.Veseli, Phys.Rev. **D62** (2000) 094021
- [24] Yu.A.Simonov, Nucl.Phys. **B307** (1988) 512;
Yu.A.Simonov and J.A.Tjon, Ann.Phys. (NY) **228** (1993) 1
- [25] H.G.Dosch, Phys.Lett. **B190** (1987) 177;
H.G.Dosch and Yu.A.Simonov, Phys.Lett. **B205** (1988) 339;
Yu.A.Simonov, Nucl.Phys. **B307** (1989) 67
- [26] Yu.A.Simonov, in *Proceedings of the XVII International School of Physics “QCD: Perturbative or Nonperturbative,”* Lisbon, 1999, edited by L.S.Ferreira, P.Nogueira and J.I.Silva-Marcos (World Scientific 2000), p. 60
- [27] A.M.Badalian, Yu.A.Simonov, Yad.Fiz. **59** (1996) 2247 (Phys.At.Nucl. **59** (1996) 2164)
- [28] E.Eichten and F.L.Feinberg, Phys.Rev. **D23** (1981) 2724;
D.Gromes, Z.Phys. **C26** (1984) 401
- [29] A.M.Badalian and B.L.G.Bakker in preparation
- [30] J.Pantaleone, S.-H.Henry Tye, Y.J.Ng, Phys.Rev. **D33** (1986) 777
- [31] Yu.A.Simonov, Nucl.Phys. **B592** (2000) 350
- [32] S.Godfrey, N.Isgur, Phys.Rev. **D32** (1985) 189;
S.Godfrey, R.Kokoski, Phys.Rev. **D43** (1991) 1679

- [33] Dan La Course and M.G.Olsson, Phys.Rev. **D39** (1989) 1751;
C.Olsson and M.G.Olsson, MAP/PH/76/(1993)
- [34] A.Le Yaouanc, L.Oliver, O.Pene and J.-C.Raynal, Phys. Rev. **D29**, 1233 (1984);
A.Le Yaouanc, L.Oliver, S.Ono, O.Pene and J.-C.Raynal, Phys.Rev. **D31** 137 (1985);
P.Bicudo and J.E.Ribeiro, Phys.Rev. **D42**, 1611 (1990);
I.Bars and M.B.Green, Phys.Rev. **D17**, 537 (1978)
- [35] Yu.S.Kalashnikova, A.V.Nefediev and A.V.Volodin, Yad.Fiz. **63** (2000) 1710 (Phys.At.Nucl. **63** (2000) 1623);
Yu.S.Kalashnikova and A.V.Nefediev, Phys.Lett. **B487** (2000) 371
- [36] Yu.A.Simonov, Z.Phys. **C53** (1992) 419
- [37] Yu.A.Simonov, Yad.Fiz. **58** (1995) 113 (Phys.At.Nucl. **58** (1995) 107); Pis'ma Zh.Eksp. Teor.Fiz. **57** (1993) 513 (JETP Lett. **57** (1993) 525)
- [38] J.Hein *et.al.*, Phys.Rev. **D62** (2000) 074503
- [39] R.Lewis, R.M.Woloshyn, Phys.Rev. **D62** (2000) 114507
- [40] D.Ebert, V.O.Galkin, R.N.Faustov, Phys.Rev. **D57** (1998) 5663
- [41] D.Melikhov and O.Pene, Phys.Lett. **B446** (1999) 336;
P.R.Page, Phys.Rev. **D60** (1999) 057501
- [42] N.Isgur, M.Wise, Phys.Lett. **B234** (1989) 113; **B237** (1990) 527
- [43] T.Mannel, *Effective Theory for Heavy Quarks*, in Lecture Notes in Physics, Vol. 479 (Springer, New York, 1996), p. 387
- [44] P.Ball and V.Braun, Phys.Rev. **D49** (1994) 2472
- [45] M.Gremm, A.Kapustin, Z.Ligeti, M.B.Wise, Phys.Lett. **B377** (1996) 20
- [46] Yu.A.Simonov, J.A.Tjon, Phys.Rev. **D62** (2000) 014501

n	0	1	2	3	4	5
$M_n(\text{WKB})$	1.373	2.097	2.629	3.070	3.455	3.802
$M_n(\text{einbein})$	1.483	2.256	2.826	3.300	3.713	4.085
$M_n(\text{combined})$	1.475	2.254	2.825	3.299	3.713	4.085
$M_n(\text{exact})$	1.412	2.106	2.634	3.073	3.457	3.803
$\frac{M_n(\text{combined}) - M_n(\text{exact})}{M_n(\text{combined})}, \%$	4.27	6.57	6.76	6.85	6.89	6.90

TABLE I. Comparison of the numerical results of the three approximate methods of solving the eigenvalues problem for equation (11) for $m = 0$, $\sigma = 0.2 \text{ GeV}^2$ and $l = 0$ given by equations (23)-(25) with the exact eigenenergies of the Hamiltonian H_1 from (22).

$n \ l$	1	2	3	4	5
0	1.719	2.029	2.287	2.516	2.725
1	2.362	2.611	2.829	3.025	3.208
2	2.850	3.069	3.264	3.442	3.608
3	3.259	3.460	3.639	3.803	3.955
4	3.619	3.806	3.973	4.127	4.268
5	3.944	4.120	4.276	4.423	4.554

TABLE II. Quasiclassical spectrum of the Hamiltonian (61), (62) for $m = 0$ and $\sigma = 0.17 \text{ GeV}^2$ minimized with respect to the einbein μ_0 (combined method).

Meson	$^{2S+1}L_J$	J^{PC}	M_{exp}, MeV	M_{theor}, MeV	$M_{theor} [32], MeV$	Error, %
ρ	3S_1	1^{--}	770	775	770	0.6
ρ_3	3D_3	3^{--}	1690	1688	1680	0.1
ρ_5	3G_5	5^{--}	2330	2250	2300	3.4
a_1	3P_1	1^{++}	1260	1346	1240	6.8
a_3	3F_3	3^{++}	2070	2021	2050	2.4
a_2	3P_2	2^{++}	1320	1316	1310	0.5
a_4	3F_4	4^{++}	2040	2002	2010	1.9
a_6	3H_6	6^{++}	2450	2491	-	1.7

TABLE III. Comparison of the masses of the light-light mesons lying on the lowest Regge trajectories ($n = 0$, $S = 1$, $J = l + 1$ for the ρ and the a_2 trajectories; $n = 0$, $S = 1$, $J = l$ for the a_1 trajectory), calculated for $\sigma = 0.17 GeV^2$ and the overall negative shifts $\sqrt{|\Delta M^2|} = 1126 MeV$ for the ρ trajectory, $\sqrt{|\Delta M^2|} = 1070 MeV$ for the a_1 trajectory, and $\sqrt{|\Delta M^2|} = 1105 MeV$ for the a_2 trajectory, with the experimental data and with the theoretical predictions taken from [32]. See also the discussion concerning the pion and the ρ -meson masses in subsection VIC.

n	l	meson	m_1	m_2	σ	α_s	λ	μ_1	μ_2	μ	E_0	$ \psi(0) $
0	0	D	1.4	0.009	0.17	0.4	0.817	1.497	0.529	0.391	2.198	0.161
		D_s	1.4	0.17	0.17	0.4	0.847	1.501	0.569	0.412	2.224	0.167
		B	4.8	0.005	0.17	0.39	0.999	4.840	0.619	0.549	5.527	0.209
		B_s	4.8	0.17	0.17	0.39	1.035	4.842	0.658	0.579	5.550	0.219
0	1	D	1.4	0.009	0.17	0.4	0.869	1.522	0.597	0.428	2.640	0
		D_s	1.4	0.17	0.17	0.4	0.891	1.525	0.629	0.445	2.663	0
		B	4.8	0.005	0.17	0.39	1.052	4.847	0.675	0.593	5.949	0
		B_s	4.8	0.17	0.17	0.39	1.080	4.849	0.707	0.617	5.970	0
0	2	D	1.4	0.009	0.17	0.4	0.924	1.554	0.674	0.470	2.961	0
		D_s	1.4	0.17	0.17	0.4	0.942	1.557	0.702	0.484	2.982	0
		B	4.8	0.005	0.17	0.39	1.128	4.860	0.762	0.659	6.245	0
		B_s	4.8	0.17	0.17	0.39	1.151	4.861	0.789	0.679	6.263	0
1	0	D	1.4	0.009	0.17	0.4	0.929	1.557	0.682	0.474	2.848	0.162
		D_s	1.4	0.17	0.17	0.4	0.947	1.561	0.710	0.488	2.869	0.165
		B	4.8	0.005	0.17	0.39	1.142	4.863	0.779	0.671	6.131	0.207
		B_s	4.8	0.17	0.17	0.39	1.165	4.864	0.806	0.692	6.149	0.212

TABLE IV. Solutions of equations (65)-(67) for standard values of the string tension σ , the strong coupling constant α_s , and the current masses of the quarks. E_0 is the mass of the corresponding state. All parameters are given in GeV to the appropriate powers.

	$n^{2S+1}L_J$	J^P	M_{exp}	M_{theor}	$M_{hl}^{(0)}$	M_{theor} [32]	M_{theor} [40]	M_{lat} [38]	M_{lat} [39]
D	1^1S_0	0^-	1869	1876	2000	1880	1875	1884	1857
D^*	1^3S_1	1^-	2010	2022	2000	2040	2009	1994	1974
D_1	$1^1P_1/{}^3P_1$	1^+	2420	<u>2354</u>	<u>2393</u>	2440/2490	2414/2501		2405/2414
				<u>2403</u>	2407				
	1^3P_0	0^+		2280	2400	2400	2438		2444
D_2	1^3P_2	2^+	2460	2432	2400	2500	2459		2445
$D^{*'} $	1^3D_3	3^-	2637	<u>2654</u>	2600	2830			
	$1^1D_2/{}^3D_2$	2^-		<u>2663</u>	2573				
				2729	2600				
	2^3S_1	0^-		<u>2664</u>	2500	2640			
D_s	1^1S_0	0^-	1968	1990	2100	1980	1981	1984	input
D_s^*	1^3S_1	1^-	2112	2137	2100	2130	2111	2087	2072
D_{1s}	$1^1P_1/{}^3P_1$	1^+	2536	<u>2471</u>	<u>2494</u>	2530/2570	2515/2569	2494	2500/2511
				<u>2516</u>	2506				
	1^3P_0	0^+		2395	2500	2480	2508		2499
D_{2s}	1^3P_2	2^+	2573	2547	2500	2590	2560	2411	2554
B	1^1S_0	0^-	5279	5277	5200	5310	5285	5293	5277
B^*	1^3S_1	1^-	5325	5340	5200	5370	5324	5322	5302
B_1	$1^1P_1/{}^3P_1$	1^+	5732	<u>5685</u>	<u>5592</u>		5719/5757		5684/5730
				<u>5719</u>	5608				
	1^3P_0	0^+		5655	5600	5760	5738		5754
B_2	1^3P_2	2^+	5731	5820	5600	5800	5733		5770
$B^{*'} $	1^3D_3	3^-	5860	<u>5955</u>	5800	6110			
	$1^1D_2/{}^3D_2$	2^-		<u>5953</u>	5773				
				6018	5827				

	2^3S_1	0^-		<u>5940</u>	5700	5930	5898	5890	
B_s	1^1S_0	0^-	5369	5377	5400	5390	5375	5383	input
B_s^*	1^3S_1	1^-	5416	5442	5400	5450	5412	5401	5395
B_{1s}	$1^1P_1/{}^3P_1$	1^+	5853	5789	5793	5860/5860	5831/5859	5783	5794/5818
				<u>5819</u>	5807				
	1^3P_0	0^+		5757	5800	5830	5841		5820
B_{2s}	1^3P_2	2^+		5834	5800	5880	5844	5848	5847

TABLE V. Masses of the D , D_s , B , and B_s mesons in MeV . For the lattice results we give only the central values extracted from Figures 26, 27 and Tables XXVIII, XXIX of [38] and from Table VIII of [39]. We also compare our results with theoretical predictions taken from [32] and [40]. The symbols $1^1P_1/{}^3P_1$ and $1^1D_2/{}^3D_2$ are used to indicate that the physical states are mixtures of the 1^1P_1 and 1^3P_1 or 1^1D_2 and 1^3D_2 states, respectively. Underlined figures give masses of the most probable candidates for the experimentally observed resonances. The column $M_{hl}^{(0)}$ contains the best fit to the experimental spectrum for the system containing one particle being infinitely heavy.

Splitting	D_s-D	$D_s^*-D^*$	D^*-D	$D_s^*-D_s$	B_s-B	$B_s^*-B^*$	B^*-B	$B_s^*-B_s$
Experiment	99	102	141	144	90	91	46	47
Theory	114	115	146	147	100	102	63	65
Theory [32]	100	90	160	150	80	80	60	60
Lattice [38]	100	92	110	103	90	90	30	29
Lattice [39]	112	98	117	103	92	93	25	29

TABLE VI. Splittings for the D , D_s , B , and B_s mesons in MeV . Lattice results are taken from Tables XXVIII, XXIX of [38] and Table VIII of [39]. We give also results of the theoretical papers [32].

	$m_1 \rightarrow \infty \ m_2 \rightarrow 0$	B mesons	Sum rules [44]	B mesons decays [45]	DS equation [46] ⁵
$\bar{\Lambda}, GeV$	0.471	0.485	$0.4 \div 0.5$	0.39 ± 0.11	0.493/0.288
λ_1, GeV^2	-0.506	-0.379	-0.52 ± 0.12	-0.19 ± 0.10	-
λ_2, GeV^2	0.21	0.17	0.12	0.12	-

TABLE VII. Standard parameters used in HQET (see equation (76)). In the first column we give the values following from formulae (80) and (82) for $\bar{\Lambda}$ and λ_2 and the corresponding one for λ_1 ; the second column contains the best fit of the form $m_Q + \bar{\Lambda} + C_0 - \frac{\lambda_1}{2m_Q}$ for the eigenvalues of the Hamiltonian (54) for m_Q in the region $4GeV < m_Q < 6GeV$ (around $m_b = 4.8GeV$), $C_0 = 203MeV$ being the overall negative shift constant taken from equation (75). The two numbers given in the last column correspond to local and nonlocal kernels of the Dyson-Schwinger (DS) equation (see [46] for details). The figures given in the first two columns correspond to $\sigma = 0.17GeV^2$ and $\alpha_s = 0.39$.

⁵Note that slightly different values for the string tension ($\sigma = 0.18GeV^2$) and the strong coupling constant ($\alpha_s = 0.3$) were used in this paper.

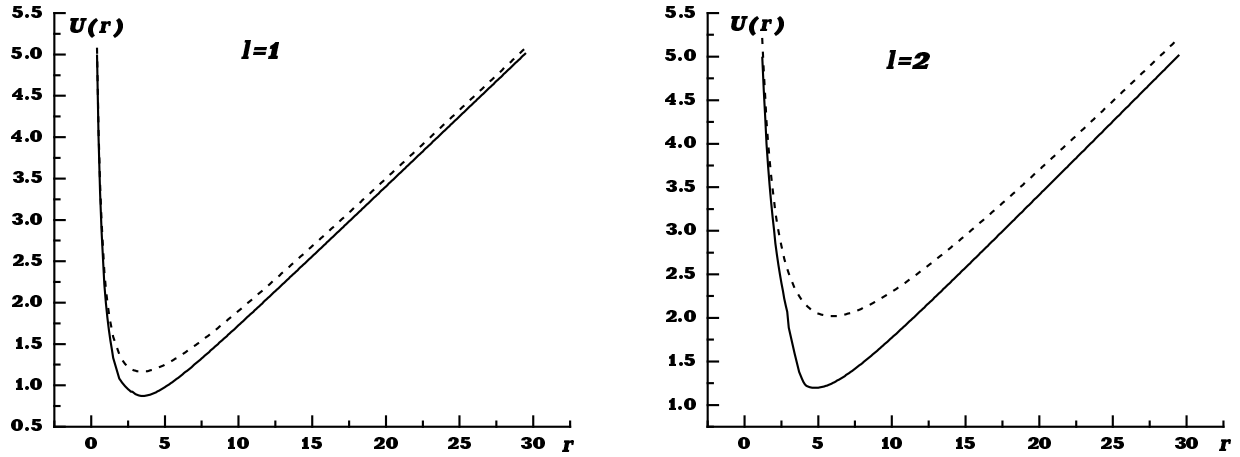


FIG. 1. Effective potential incorporating the string rotation as well as the quark radial motion for $\sigma = 0.17 \text{ GeV}^2$ and two values of the angular momentum l (solid line). The naive sum of the quark centrifugal barrier for the given l and the linearly rising potential σr is given in each graph by the dotted line. For $l = 0$ the effective potential coincides with σr for all values of r .

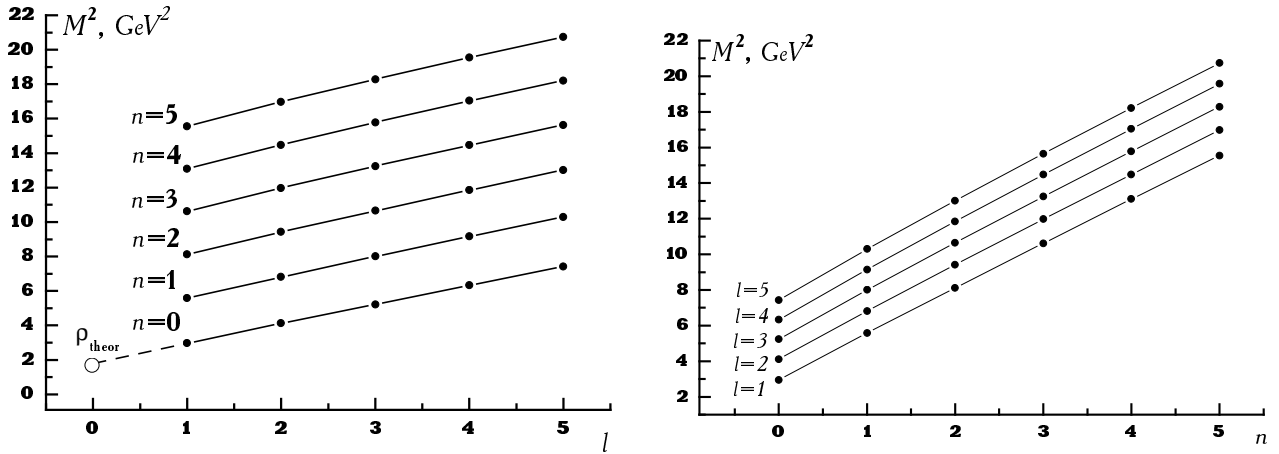


FIG. 2. The Regge trajectories for the Hamiltonian (56) for $m = 0$ and $\sigma = 0.17 \text{ GeV}^2$ (see Table II). Theoretical prediction for the ρ -meson mass ($M_\rho^2 \approx 1.7 \text{ GeV}^2$; see the column in Table I for $n = 0$) is shown not to violate the straight-line behaviour of the leading theoretical trajectory (see left plot).

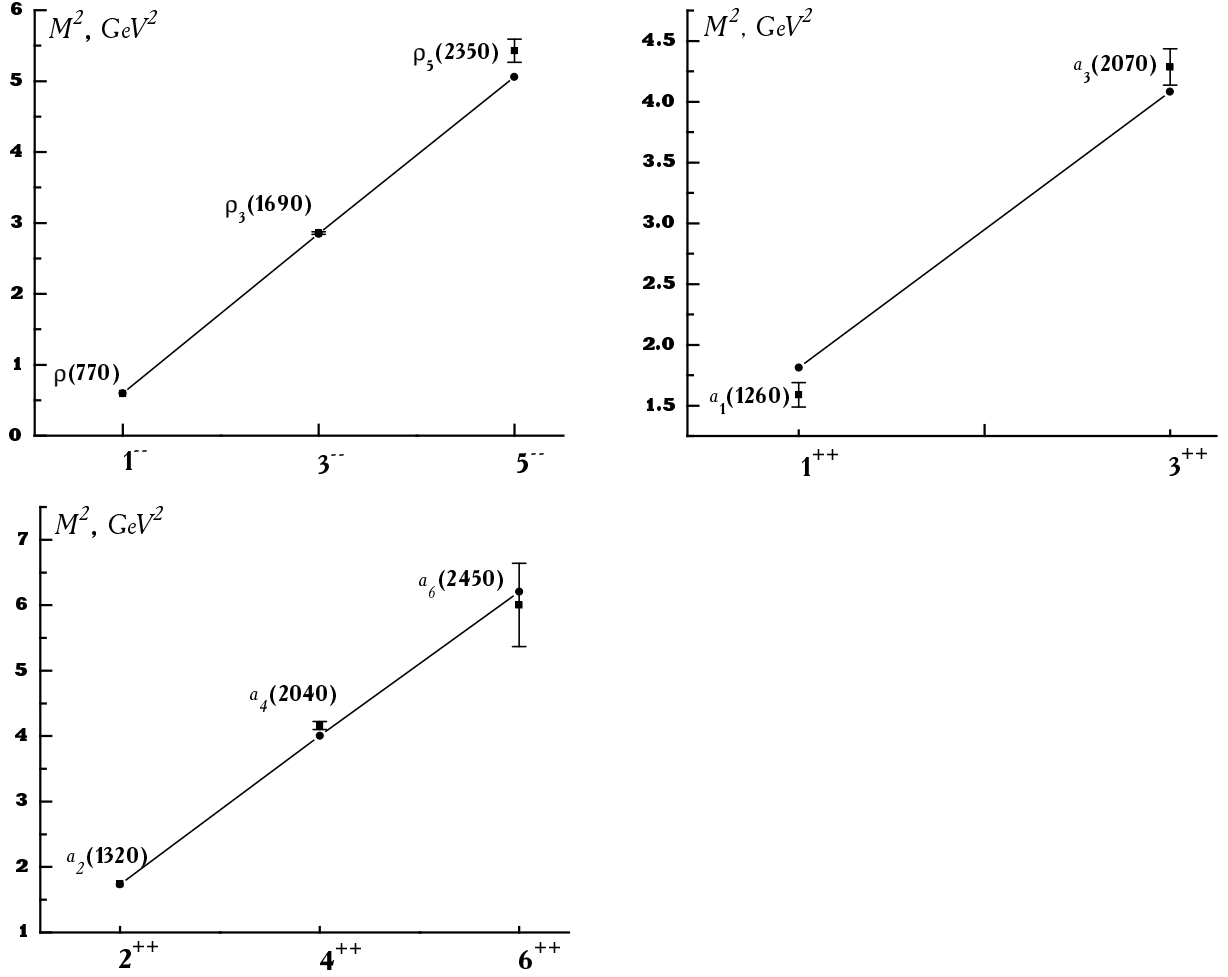


FIG. 3. The lowest Regge trajectories for light–light mesons fitted with respect to the overall negative mass shift (see Table III). The theoretical values for $m = 0$ and $\sigma = 0.17 \text{ GeV}^2$ are marked with dots; the experimental data are given by boxes with error bars.